# Synthesis, characterization and photo catalytic degradation of aqueous eosin over Cr containing Ti/MCM-41 and SiO$_2$-TiO$_2$ catalysts using visible light

S.V. Awate, N.E. Jacob, S.S. Deshpande, T.R. Gaydhankar, A.A. Belhekar[*]

*Catalysis Division, National Chemical Laboratory, Pashan, Pune 411008, India*

## Abstract

Two series of samples were prepared namely Cr-Ti/MCM-41 and Cr/SiO$_2$-TiO$_2$ keeping Si/Ti mole ratio same, with different Cr loading. The physico-chemical properties of the samples were characterized by different analytical techniques such as XRD, FTIR, TEM, low temperature N$_2$ sorption, and UV–vis diffused reflectance spectroscopy. The impregnated TiO$_2$ was in anatase form. The crystallite size was determined from Scherrer equation as well as by TEM. There is a difference between the shapes of nitrogen adsorption isotherms with and without Cr-loaded Ti/MCM-41 samples. The rate of nitrogen adsorption was found to increase with decrease in Cr content at lower $P/P_0$ for Cr-Ti/MCM-41 samples due to the blocking of the pores with Cr. All MCM-41 samples exhibited pore sizes from 24 nm to 32 nm. UV–vis diffused reflectance spectra of all Cr-loaded samples showed red shift of their absorption edges. Photo degradation of eosin dye was studied using visible light.
© 2004 Elsevier B.V. All rights reserved.

*Keywords:* Cr-Ti/MCM-41; Cr/SiO$_2$-TiO$_2$; Photo degradation; Eosin; Visible light

## 1. Introduction

Today, the whole world is facing with a tremendous set of environmental problems which are due to contaminated ground water, hazardous waste effluent coming out of industrial sectors due to advanced industrialization in different fields. Heterogeneous photo catalytic purification of water by irradiating semiconductor TiO$_2$ with UV light has been found to be very effective process for complete mineralization of organic molecules dissolved in water [1–4]. It is known that only 5% of the total solar energy reaching the earth is UV. The use of artificial UV light for photo degradation purpose is expensive due to the requirement of the additional power supply. So, there are limitations for the use of TiO$_2$ in the treatment of wastewater using UV light from practical point of view.

TiO$_2$ has an absorption edge in the UV region. When they are substituted by transition metals [5,6] like Fe, V, Cr, their absorption edges shift in the visible light. So, modified titanium dioxide doped with transition metals [6] was also studied for the degradation in visible light. Different semiconductors such as TiO$_2$, CdS, ZnO, Fe$_2$O$_3$, ZnS, etc. are reported as photo catalysts till today and have their own merits and demerits in visible light [7]. Enhanced photo catalytic activity of titania supported on molecular sieves has been reported [3,7]. Davydov et al. [7] have reported titania loaded transition metal-substituted MCM-41 molecular sieves as potential catalysts for the oxidation of organics in visible light.

TiO$_2$ has been used extensively for degradation of organic pollutants and dyes in wastewater treatment. Practically separation of TiO$_2$ from water is expensive due to formation of milky dispersions after mixing the powder in water. Silica has been used selectively and widely as a support in industry for a variety of reactions as it does not possess a charge framework [8,9]. Transition metals-loaded silica-titania are also studied

* Corresponding author. Tel.: +91 20 5893300; fax: +91 20 5893761.
*E-mail address:* Belhekar@cata.ncl.res.in (A.A. Belhekar).

extensively for their physico-chemical properties and photo catalytic activity [10].

TiO$_2$, though most durable photo catalyst, is active only in UV light, while others are active in visible light but have low stability. Overall, there has been no photo catalyst prepared which can be used in visible light having both chemical stability and high photo activity. So, there is an urgent need for developing a new photo catalyst, which is chemically stable, active in visible light, economic, and ecofriendly also.

Our aim is to prepare the catalysts, which are active in visible light so that they can allow more effective utilization of solar energy. We wish to report herein the preparation, characterization and catalytic evaluation of titania loaded on MCM-41, doped with Cr. Also, silica-titania catalysts were prepared keeping Si/Ti mole ratio equal to that in Ti/MCM-41 and doped with Cr. Eosin was selected as a pollutant for the photo catalysis.

## 2. Experimental

### 2.1. Synthesis

The synthesis of Si-MCM-41 was carried [11] out using the molar gel composition 1SiO$_2$:0.25 TMAOH:0.18 CTMABr:25 H$_2$O at ambient temperature 383 K. 3.560 g *N*-cetyl-*N,N,N*-trimethyl ammonium bromide (CTABr; Loba chemie, 99.8%) was dissolved in 5 g of distilled water (solution I). 4.945 g of tetra methyl ammonium hydroxide (TMAOH; Loba chemie, 25%) was dissolved in 5 g distilled water (solution II). 3.256 g of fumed silica (Aldrich, 99.8%) was added slowly to solution II with constant stirring for 2 h. Then solution I was added to the above mixture to get thick gel, which was stirred for 2 h. Then, 5.237 g of water was added again and the gel was stirred for another half an hour. The gel was then transferred to stainless steel autoclave and kept in an oven at 383 K till fully crystalline material is obtained as checked with XRD. Then the sample was filtered, washed thoroughly with cold distilled water and then with about 50 ml acetone. The material was then dried in an oven at 373 K and calcined stepwise up to 813 K and kept for 4 h.

### 2.2. Preparation of titania-loaded MCM-41, doped with Cr

To the mixture of titanium isopropoxide (Aldrich) in isopropanol and CrCl$_3$, MCM-41 powder was added under stirring for about 1 h at ambient temperature, keeping Si/Ti mole ratio 10 and Cr content ranging from 0 to 10%. The solution was allowed to dry at room temperature and then the catalyst was calcined in the range 623–773 K for 4 h.

### 2.3. Preparation of silica-titania catalyst, doped with Cr

Cr-doped SiO$_2$-TiO$_2$ catalyst was prepared by sol–gel method keeping Si/Ti mole ratio 10 and Cr content ranging from 0 to 10% using titanium isopropoxide, tetraethyl ortho silicate in isopropanol and CrCl$_3$. The solution was stirred for 1 h, dried and calcined at 773 K for 4 h.

### 2.4. Characterization

Catalysts were examined for their structural, textural, optical and photo catalytic properties by different analytical techniques. XRD powder diffraction spectra of the calcined samples were recorded on Rigaku (D Max III VC) using Cu K$\alpha$ radiation ($\lambda = 1.5406$ Å) over the scan range $2\theta = 3°$ to 80°. The crystallite size of the anatase was determined by applying Scherrer equation to XRD data. TEM images were obtained on JEOL-2010 CX microscope. From low temperature nitrogen adsorption (Quantachrome NOVA 1200) isotherms BET surface area, pore diameter, total pore volume, micropore volume and pore size distribution was determined. Prior to the determination of adsorption isotherm, the sample was evacuated at $10^{-2}$ Torr and at 573 K to remove all physisorbed species from the surface of the adsorbent. The samples were further characterized by UV–vis diffuse reflectance spectroscopy (Shimadzu UV-2550 UV–vis spectrophotometer) using barium sulfate as a standard. FTIR spectra were recorded in nujol matrix using Shimadzu 8300 FTIR spectrometer.

### 2.5. Photocatalysis

For photo-catalytic oxidation of the eosin, halogen lamp (500 W) was used for photo-irradiation. 125 mg of the calcined sample was dispersed in 350 ml of $2 \times 10^{-5}$ M aqueous dye solution in a photo reactor and stirred magnetically in dark for 60 min. The absorbance measurement was done at $\lambda_{max} = 520$ nm for eosin using UV–vis spectrometer, Shimadzu UV-2101PC. The mixture of the sample and dye solution was then photo-irradiated/not irradiated at room temperature for 10 min, centrifuged to get clear solution and absorbance of clear solution was measured. This procedure was consecutively repeated several times without changing the concentration of reaction mixture.
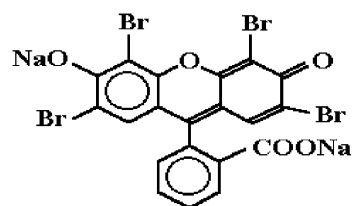


*Structure of eosin

## 3. Results and discussion

Two sets of samples were prepared namely Cr-Ti/MCM-41 and Cr/SiO$_2$-TiO$_2$ keeping Si/Ti mole ratio 10 and with different Cr loading ranging from 0 to 10%. The sample

Table 1
Structural and textural properties of catalysts derived from nitrogen sorption studies

| No. | Sample | $TiO_2$ particle diameter[a] (nm) | BET specific surface area[b] ($m^2/g$) | Total pore volume[c] ($cm^3/g$) | Micropore volume ($cm^3/g$) | Average pore diameter (Å) |
|---|---|---|---|---|---|---|
| 1. | Cr-Ti/MCM-41 (0) | 19.2 | 798 | 0.6452 | 0.4567 | 32.3 |
| 2. | Cr-Ti/MCM-41 (2.5) | 11.5 | 549 | 0.4133 | 0.2811 | 24.8 |
| 3. | Cr-Ti/MCM-41 (5) | 9.1 | 540 | 0.3490 | 0.2284 | 25.9 |
| 4. | Cr-Ti/MCM-41 (10) | >100 | 328 | 0.2240 | 0.1369 | 27.3 |
| 5. | Cr/SiO$_2$-TiO$_2$ (0) | 19 | 5 | – | – | – |
| 6. | Cr/SiO$_2$-TiO$_2$ (2.5) | 23 | <3 | – | – | – |
| 7. | Cr/SiO$_2$-TiO$_2$ (5) | 19 | <3 | – | – | – |
| 8. | Cr/SiO$_2$-TiO$_2$ (10) | 25 | 5 | – | – | – |

The figures in the bracket ( ) correspond to %Cr.
  [a] Determined by Scherrer's equation with (1 0 1) reflection on XRD pattern.
  [b] Determined from nitrogen isotherm.
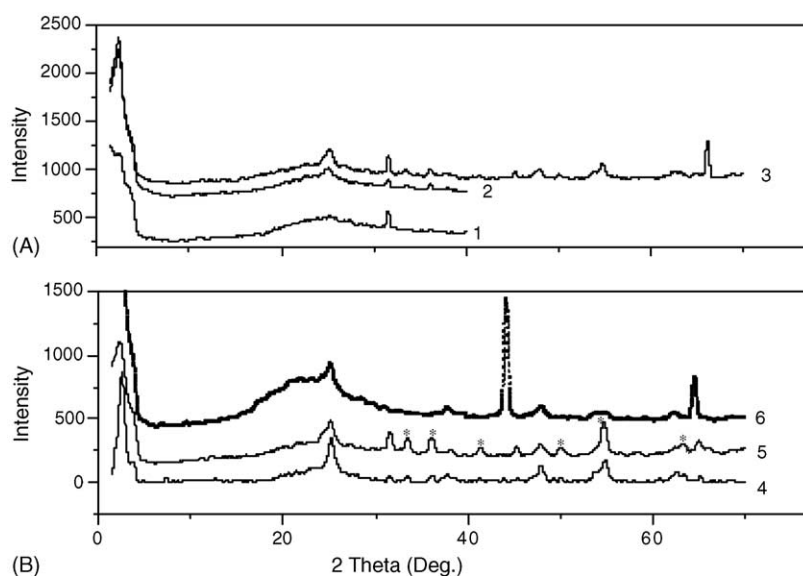  [c] Determined from T plot.



Fig. 1. XRD profiles of (A)—Cr-Ti/MCM-41 (5) samples calcined at different temperatures [1] 623 K for 4 h, [2] 623 K for 20 h and [3] 773 K for 4 h; and (B)—[4] Cr-Ti/MCM-41 (2.5), [5] Cr-Ti/MCM-41 (10) and [6] Cr-Ti/MCM-41 (0) samples calcined at 773 K for 4 h.

designations, structural and textural properties of the samples are listed in the Table 1. Fig. 1A depicts the powder XRD profiles 1–3 of Cr-Ti/MCM-41 (5) samples calcined at 623 K (4 h), 623 K (20 h) and 773 K (4 h), respectively. It is seen that sample calcined at 623 K for 4 h is amorphous and transforms into anatase with visualization of peaks at $2\theta = {\sim}25°, 48°, 55°$ and $63°$ for samples calcined at 623 K (20 h) and 773 (4 h). Further heating the sample above 773 K, rutile phase starts appearing (graph not shown). XRD profiles of Cr-Ti/MCM-41 (0), Cr-Ti/MCM-41 (2.5) and Cr-Ti/MCM-41 (10) samples calcined at 773 K for 4 h are shown in Fig. 1B.

Fig. 2 gives the XRD profiles of Cr/SiO$_2$-TiO$_2$ (0), Cr/SiO$_2$-TiO$_2$ (2.5), Cr/SiO$_2$-TiO$_2$ (5) and Cr/SiO$_2$-TiO$_2$ (10) samples calcined at 773 K for 4 h. All the samples show anatase peaks. The TiO$_2$ particle diameter estimated with Scherrer's equation using the line-width at half-maximum of the X-ray diffraction peaks at $2\theta = 25.4$ for anatase was found to be in the range 9–25 nm for all the samples except
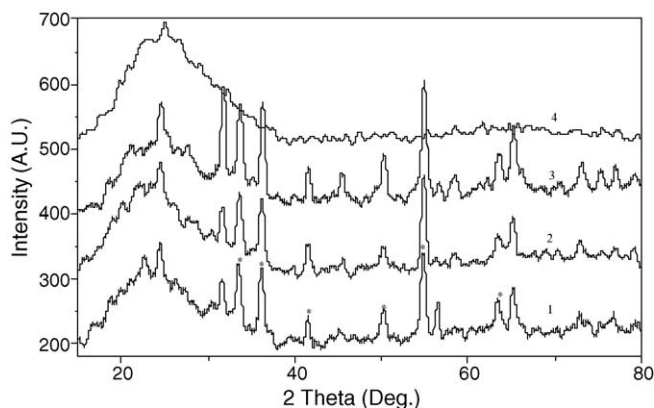


Fig. 2. XRD profiles of [1] Cr/SiO$_2$-TiO$_2$ (2.5), [2] Cr/SiO$_2$-TiO$_2$ (5), [3] Cr/SiO$_2$-TiO$_2$ (10), [4] Cr/SiO$_2$-TiO$_2$ (0) samples calcined at 773 K for 4 h.
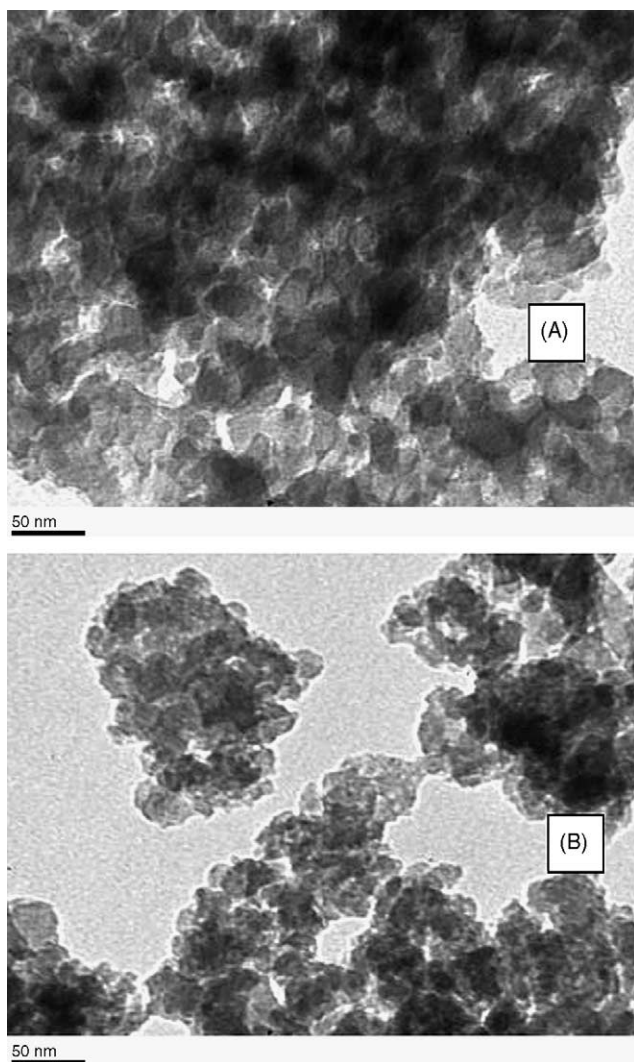
Fig. 3. Transmission electron micrographs of (A)—Cr-Ti/MCM-41 (5); and (B)—Cr/SiO$_2$-TiO$_2$ (5).



Fig. 4. Nitrogen adsorption–desorpti on isotherms for calcined [1] Cr-Ti/MCM-41 (2.5), [2] Cr-Ti/MCM-41 (5) and [3] Cr-Ti/MCM-41 (10) and [4] Cr-Ti/MCM-41 (0). The inset shows the BJH pore size distribution curves.

Cr-Ti/MCM-41 (10). The mark '*' denotes the peaks due to chromium oxide for all the samples.

Fig. 3A and B show TEM photographs of Cr-Ti/MCM-41 (5) and Cr/SiO$_2$-TiO$_2$ (5) samples. Small dark spots representing TiO$_2$ has the particle size around 3 nm and 6 nm, respectively. The crystallite size of the same samples calculated from XRD is 9.1 nm and 19 nm, respectively, which is generally higher than that observed by TEM. This can be because XRD patterns can show only titania species of sufficient size, i.e around 2 nm [12]. While TEM images show additionally non-crystalline species also. This could explain the different crystallite sizes found with both the techniques.

Fig. 4 shows adsorption-desorption isotherms of nitrogen at 77 K on Cr-Ti/MCM-41 (0), Cr-Ti/MCM-41 (2.5), Cr-Ti/MCM-41 (5), Cr-Ti/MCM-41 (10). The isotherm of Cr-Ti/MCM-41 (0) can be classified as type IV according to the IUPAC convention [13] and is typical of mesoporous material. For all the samples, a linear increase at low relative
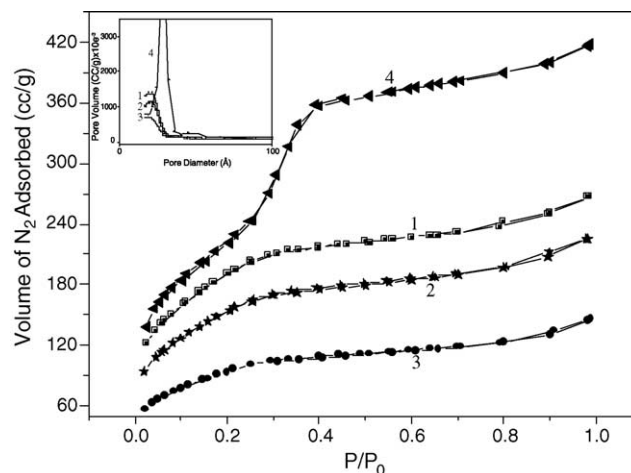
pressure of nitrogen up to $P/P_0 = 0.25$ indicates monolayer nitrogen adsorption in the mesoporous pores. The rate of nitrogen adsorption was found to increase with decrease in Cr content at lower $P/P_0$. This may be due to blocking of the pores with higher Cr loading. This is reflected in decrease in total pore volume and micropore volume with increase in Cr loading as shown in Table 1. The BET surface area was also found to decrease with increase in Cr loading. At higher relative pressure >0.25, a steep rise in nitrogen uptake for Cr-Ti/MCM-41 (0) is due to capillary condensation inside the mesoporous pores [14]. Cr containing samples however showed gradual uptake at higher relative pressure. Thus, there is difference between the shapes of the Cr loaded and without loaded Ti/MCM-41 samples. The specific surface areas of Cr-Ti/MCM-41 samples are shown in Table 1. It decreases as Cr loading increases due to blocking of pores by Cr. It was observed that the pore size of the Cr-loaded samples (inset figure) decreased compared to the sample without Cr. The pore size was reduced to about 15–25% with Cr loading. Since area of all Cr/SiO$_2$-TiO$_2$ samples was very less, total pore volume, total micropore volume and average pore diameter of these samples were not determined.

Fig. 5 shows FTIR spectra of Cr-Ti/MCM-41 (0), Cr-Ti/MCM-41 (2.5), Cr/SiO$_2$-TiO$_2$ (0) and Cr/SiO$_2$-TiO$_2$ (2.5). The shoulder at 880–900 cm$^{-1}$ in Cr-containing samples can be assigned to Cr=O or Cr–O vibration from Cr (VI) species as reported earlier [15]. This absorption is absent in samples without Cr. The peaks near 1089 and 802 cm$^{-1}$ correspond to asymmetric and symmetric vibrations of Si–O–Si linkage, respectively. The peak at 464 cm$^{-1}$ has been ascribed to bending vibration of Si–O–Si linkage. The band at 952 cm$^{-1}$ can be assigned to Si–O–Ti vibration, which is also assigned to lattice defect and is correlated to the presence of Cr as well as Ti ions [16]. The bands at 623 and 569 cm$^{-1}$ are found to be due to extra framework chromium oxide as reported earlier
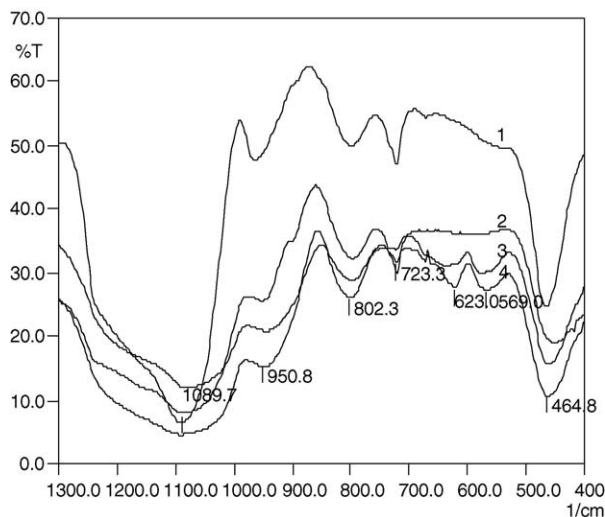
Fig. 5. FTIR spectra of [1] Cr-Ti/MCM-41 (0), [2] Cr/SiO$_2$-TiO$_2$ (0), [3] Cr-Ti/MCM-41 (2.5), and [4] Cr/SiO$_2$-TiO$_2$ (2.5).

[17]. These bands are found to be absent in Cr-Ti/MCM-41 (0) and Cr/SiO$_2$-TiO$_2$ (0) where Cr is not impregnated.

UV–vis diffused reflectance spectra of Cr-Ti/MCM-41 (0), Cr-Ti/MCM-41 (2.5), Cr-Ti/MCM-41 (5) and Cr-Ti/MCM-41 (10) are shown in Fig. 6A. Ti/MCM-41 without Cr shows completely different spectrum as compared to those

with Cr. It resembles to the spectrum of TiO$_2$. Cr-containing samples show three absorption edges ∼300, 450 and 550 nm and first due to the charge transfer O→Cr, second due to heteroconjugation of TiO$_2$ with transition metal and the last due to d–d transition in metal oxide [7,18]. UV–vis diffused reflectance spectra of Cr/SiO$_2$-TiO$_2$ (0), Cr/SiO$_2$-TiO$_2$ (2.5), Cr/SiO$_2$-TiO$_2$ (5), Cr/SiO$_2$-TiO$_2$ (10) are shown in Fig. 6B. The spectrum of Cr/SiO$_2$-TiO$_2$ (0) resembles the spectrum of TiO$_2$ showing no absorption in the visible region. All Cr-containing samples show three absorption edges as above.

### 3.1. Photo degradation activity of eosin

In order to test the photo catalytic degradation activity of the catalysts, eosin dye was selected. Fig. 7A and B depicts the photo catalytic degradation activity of eosin on Cr-Ti/MCM-41 (0), Cr-Ti/MCM-41 (2.5), Cr-Ti/MCM-41 (5), Cr-
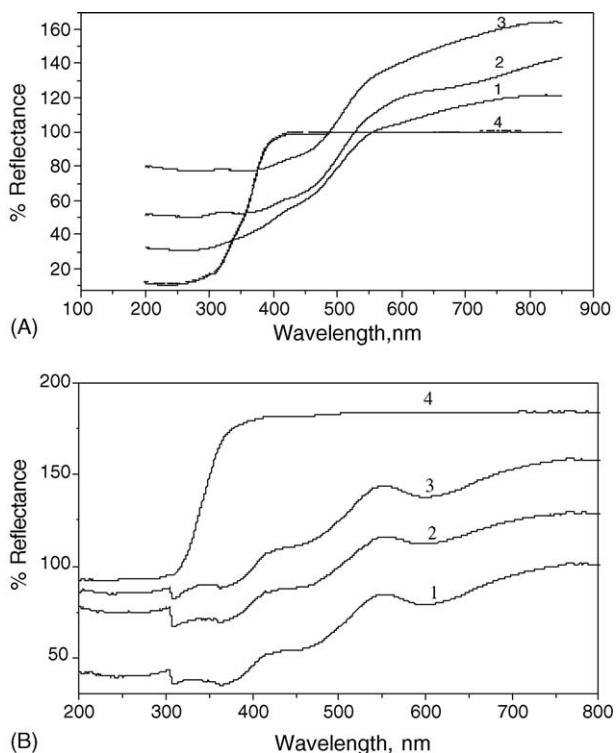


Fig. 6. UV–vis spectra of samples (A)—1: Cr-Ti/MCM-41 (2.5), 2: Cr-Ti/MCM-41 (5), 3: Cr-Ti/MCM-41 (10), 4: Cr-Ti/MCM-41 (0) calcined at 773 K for 4 h; and (B)—1: Cr/SiO$_2$-TiO$_2$ (2.5), 2: Cr/SiO$_2$-TiO$_2$ (5), 3: Cr/SiO$_2$-TiO$_2$ (10), 4: Cr/SiO$_2$-TiO$_2$ (0) calcined at 773 K for 4 h.
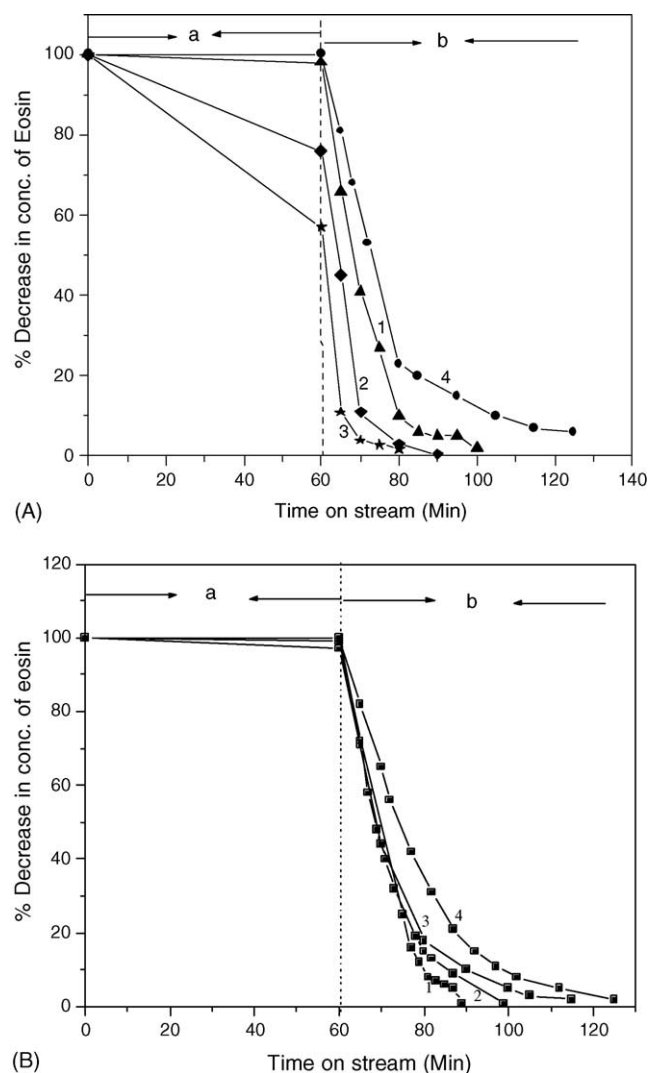


Fig. 7. Photo catalytic degradation of eosin on (A)—1: Cr-Ti/MCM-41 (2.5), 2: Cr-Ti/MCM-41 (5), 3: Cr-Ti/MCM-41 (10), 4: Cr-Ti/MCM-41 (0) calcined at 773 K for 4 h; and (B)—1: Cr/SiO$_2$-TiO$_2$ (2.5), 2: Cr/SiO$_2$-TiO$_2$ (5), 3: Cr/SiO$_2$-TiO$_2$ (10), 4: Cr/SiO$_2$-TiO$_2$ (0) calcined at 773 K for 4 h.

Ti/MCM-41 (10) and Cr/SiO$_2$-TiO$_2$ (0), Cr/SiO$_2$-TiO$_2$ (2.5), Cr/SiO$_2$-TiO$_2$ (5), Cr/SiO$_2$-TiO$_2$ (10), respectively. Period 'a' is the initial time (60 min for all the samples) for which the mixture of sample and the eosin solution is stirred in dark and 'b' denotes the results obtained after interval of time after exposing the reaction mixture to visible radiation. As seen in Fig. 7A, all the samples show decrease in concentration of dye in dark (100, 98, 76, 57%) with increase in Cr loading (0, 2.5, 5, 10%, respectively), even though BET surface area, total pore volume and micropore volume was found to decrease with increase in Cr content. Cr content may be enhancing the adsorption of eosin in all Cr-Ti/MCM-41 samples. It was observed that the rate of photo degradation for samples containing Cr was higher than the sample without Cr. For Cr-Ti/MCM-41 with 0, 2.5, 5 and 10% Cr loading the decrease in concentration of eosin was found to be 23, 10, 8.5 and 2%, respectively, at the end of 20 min of visible light irradiation. For Cr-Ti/MCM-41 (5) and Cr-Ti/MCM-41 (10) samples, the decrease in concentration of eosin was faster compared to gradual decrease in concentration of eosin for Cr-Ti/MCM-41 (2.5). The photo degradation activity of eosin over Cr-Ti/MCM-41 (0) sample may be due to sensitized photo catalysis reaction mechanism [19]. But the amount of Cr definitely affects the rate of photo degradation activity of eosin.

The reaction mixture was tested for Cr and Ti after the experiment by atomic absorption spectroscopy. There was 0 and 20% Cr leaching for 2.5 and 10% Cr-loaded samples, respectively. Ti leaching was not observed for all the samples.

In course of reaction, absorbance measurement of the solution in the visible and ultraviolet regions, showed no new bands of aromatic moieties and other similar intermediates indicating mineralization of eosin. After complete decolourization, the reaction mixture of all the samples was extracted with diethyl ether and analyzed on GC. GC spectra showed complete degradation of the pollutant and also complete mineralization of the dye molecules.

As seen in Fig. 7B, Cr-containing SiO$_2$-TiO$_2$ samples show negligible adsorption of dye molecules in dark. Higher adsorption of dye in all Cr-containing Ti/MCM-41 samples may be due to well dispersion of Cr over higher surface area. At the end of 20 min of visible light irradiation, the decrease in concentration of eosin was 35, 17.5, 15 and 11% over Cr/SiO$_2$-TiO$_2$ with 0, 2.5, 5 and 10% Cr loading, respectively.

All Cr-containing Ti/MCM-41 samples show greater activity for the adsorption as well as degradation of eosin compared to corresponding SiO$_2$-TiO$_2$ samples containing same amount of Cr. This may be due to higher surface area and well dispersion of Cr over Ti/MCM-41 samples.

Zhang et al. [3] have studied degradation kinetics of eosin in TiO$_2$ (Degussa) dispersions under visible light irradiation. TiO$_2$ (Degussa) took about 63 min visible irradiation for 50% decrease in concentration of eosin to initial concentration. Whereas all Cr containing Ti/MCM-41 and SiO$_2$-TiO$_2$ samples took few seconds to 8 min and 8–10 min, respectively, for 50% decrease in concentration of eosin. Zhang et al. [3] observed no degradation of eosin ($2 \times 10^{-5}$ mole l$^{-1}$) in dark and with exposure to visible light (>470 nm), it took almost 10 h for complete degradation. All Cr-Ti/MCM-41 and Cr/SiO$_2$-TiO$_2$ samples took 20–40 min and 30–60 min for complete degradation of eosin.

## 4. Conclusions

Cr-Ti/MCM-41 and Cr/SiO$_2$-TiO$_2$ samples were prepared keeping Si/Ti mole ratio same, with different Cr loading. XRD revealed that in all samples, TiO$_2$ was in anatase form with crystallite size in the range 9–25 nm determined from Scherrer equation except for Cr-Ti/MCM-41 (10). There is a difference between the shapes of nitrogen adsorption isotherms with and without Cr-loaded Ti/MCM-41 samples. All Cr-Ti/MCM-41 samples exhibited pore sizes from 24 nm to 32 nm. FTIR spectra of Cr-loaded samples show peaks at 623 and 569 cm$^{-1}$ due to extra framework chromium oxide. UV–vis diffused reflectance spectra of all Cr-loaded samples show red shift of their absorption bands. Photo degradation of eosin dye was studied using visible light. Among two sets of catalysts prepared in present studies all, Cr-Ti/MCM-41 samples showed comparatively better activity for degradation of eosin than corresponding all Cr/SiO$_2$-TiO$_2$ samples under visible light.

## References

[1] M. Anpo, Pure Appl. Chem. 72 (7) (2000) 1265.
[2] A.A. Belhekar, S.V. Awate, R. Anand, Catal. Commun. 3 (2002) 453.
[3] F. Zhang, J. Zhao, T. Shen, H. Hidaka, E. Pelizzetti, N. Serpone, Appl. Catal. B: Environ. 15 (1998) 147.
[4] J.M. Hermann, Water treatment by heterogeneous photo catalysis, in: Environmental Catalysis, F.J.J.G., Janssen, R.A., van Santen (Eds.), Catalysis Science Series, vol. I, Imperical College Press, London, 1999, pp. 171–194 (Chapter 9).
[5] K.R. Gopidas, P.V. Kamat, J. Phys. Chem. 93 (1989) 6433.
[6] H. Yamashita, M. Harada, J. Misaka, M. Takeuchi, B. Neppolian, M. Anpo, Catal. Today 84 (2003) 191.
[7] L. Davydov, E.P. Reddy, P. France, P.G. Smirniotis, J. Catal. 203 (2001) 157.
[8] C. Hu, Y. Tang, J.C. Yu, P.K. Wong, Appl. Catal. B: Environ. 40 (2003) 131.
[9] C. Hu, Y. Wan, H. Tang, Appl. Catal. B: Environ. 30 (2001) 277.
[10] X. Ga, I.E. Wachs, Catal. Today 51 (1999) 233.
[11] S.C. Laha, R. Kumar, Micropor. Mesopor. Mater. 53 (2002) 163.
[12] Y.H. Hsien, C.F. Chang, Y.H. Chen, S. Cheng, Appl. Catal. B 31 (2001) 241.
[13] S. Zheng, L. Gao, Q. Zhang, J. Guo, J. Mater. Chem. 10 (2000) 723.
[14] M. Kruk, M. Jaroniec, Y. Sakamoto, O. Terasaki, R. Ryoo, C.H. Ko, J. Phys. Chem. B 104 (2000) 292.
[15] M.A. Vuurman, I.E. Wachs, D.J. Stufkens, A.J. Oskam, Mol. Catal. 80 (1993) 209.
[16] T. Chapus, A. Tuel, Y. Taarit, C. Naccache, Zeolites 14 (1994) 349.
[17] J.A. Gadsden, Infrared Spectra of Minerals and Related Inorganic Compounds, Butterworth and Co. Publishers Ltd., 1975, pp. 44.
[18] Z.D. Zhu, Z.X. Chang, L. Kevan, J. Phys. Chem. B 103 (1999) 2680.
[19] Y. Xie, C. Yuan, J. Mol. Catal. A: Chem. 206 (2003) 419.